

Photovoltaic Characteristics of ZnO Nanotube Dye-Sensitized Solar Cells and TiO₂ Nanostructure.

Yahia Chergui*, Nadia Nehaoua, and DE Mekki

LESIMS Laboratory, Department of physics, Badji Mokhtar's, University, Annaba, Algeria.

Research Article

Received: 11/08/2013

Revised: 16/09/2013

Accepted: 02/10/2013

*For Correspondence

LESIMS Laboratory, Department of physics, Badji Mokhtar's, University, Annaba, Algeria.

Keywords: Nanotube, Titanium, oxide Zinc, simulation, photovoltaic, physical parameters

ABSTRACT

The electrical transport in nanotube is extremely sensitive to local electrostatic environment due to their small size, large surface to volume ratio and high mobility. Among them, Oxide Zinc and Titanium are friendly for environment and promised materials. Dye sensitized solar cell (DSSC) is the only solar cell that can offer both the flexibility and transparency but its conversion efficiency is affected by physical and morphological parameters, like thickness, series resistance (R_s), ideality factor (n), saturation current (I_s), shunt resistance (R_{sh}) and photocurrent (I_{ph}) during elaboration as well as their normal use. This paper presents a simulation of photovoltaic characteristics of ZnO nanotube dye-sensitized solar cells and TiO₂ nanostructure, by extracting the solar cell parameters which influence directly on solar cell output: conversion efficiency, fill factor, the short circuit photocurrent densities I_{sc} and open-circuit voltage V_{oc} . Furthermore, we review the relationship between geometry and output parameters.

INTRODUCTION

In recent decades, dye-sensitized solar cells (DSSCs) have attracted much attention as next-generation solar cells due to their remarkably high conversion efficiency combined with their ease and low cost of manufacturing. It is based on solar light harvesting of a sensitizing dye (SD) attached to a wide band gap semiconductor. The process of conversion of solar energy to electrical energy in a DSSC involves SD adsorbed on the surface of wide band gap n-type metal oxide semiconductor nanoparticles^[1] (typically TiO₂, ZnO, SnO₂, Nb₂O₅, etc).

The oxide material of choice for many of these systems has been TiO₂. Its properties are intimately linked to the material content, chemical composition, structure and surface morphology. From the point of the material content and morphology, two crystalline forms of TiO₂ are important, anatase and rutile (the third form, brookite, is difficult to obtain). Anatase is the low temperature stable form and gives mesoscopic films that are transparent and colorless^[2,3,4,5].

The application of ZnO in excitonic solar cells, XSCs, (organic, dye sensitized and hybrid) has been rising over the last few years due to its similarities with the most studied semiconductor oxide, TiO₂. ZnO presents comparable band gap values and conduction band position as well as higher electron mobility than TiO₂. It can be synthesized in a wide variety of nanoforms applying straight forward and scalable synthesis methodologies^[6,7,8,9,10]. Particularly, the application of vertically-aligned ZnO nanostructures it is thought to improve contact between the donor and acceptor material in organic solar cells (OSCs), or improve electron injection in dye sensitized solar cells (DSSCs).

Since the invention of dye sensitized solar cells (DSSC)^[11], some significant progresses have enabled to reach an efficiency higher than 11% for this type of solar cells^[12]. Until now, the major part of the photoanode DSSC research has mainly focused on TiO₂ nanostructures. However, ZnO semiconductor can be a good alternative as it can exhibit several advantages in comparison with TiO₂ semiconductor, such as a direct band gap (3.37 eV), higher exciton binding

energy (60 meV) compared to TiO₂ (4 meV), and higher electron mobility (200 cm² V⁻¹ s⁻¹) over TiO₂ (30 cm² V⁻¹ s⁻¹) for similar band gap energy levels^[13,14]. Furthermore, several types of ZnO nanostructures with different geometries can easily be grown, such as nanoparticles, nanowires, nanorods, or nanobelts^[15,16,17,18]. Nevertheless, the solar energy conversion efficiencies are twice lower for ZnO based solar cells than for TiO₂ based solar cells for some reasons which are still unidentified.

These work, present a comparative study between ZnO nanotube and TiO₂ nanostructure dye-sensitized solar cell (DSSC) by extracting the solar cell parameters which influence directly on solar cell output: conversion efficiency, fill factor, the short circuit photocurrent densities I_{sc} and open-circuit voltage V_{oc}. Furthermore, the geometry parameters of the basic material play an important role in physical parameters and output parameters, so, we review the relationship between output parameters and geometry parameter.

MATERIALS AND METHODS

Solar Cell Model

The model of the solar cells for which the superposition principle is applicable can be represented by expressed as Eq.(1) which includes light-generating current source (I_{ph}), series resistance (R_s) and shunt resistance (R_{sh}).

$$I = I_{ph} - I_d - I_p$$

$$= I_{ph} - I_s \left[\exp\left(\frac{\beta}{n}(V + IR_s)\right) - 1 \right] - G_{sh}(V + IR_s) \quad (1)$$

I_{ph}, I_s, n, R_s and G_{sh} (=1/R_{sh}) being the photocurrent, the diode saturation current, the diode quality factor, the series resistance and the shunt conductance, respectively. I_p is the shunt current and β=q/kT is the usual inverse thermal voltage.

Measurement data provided by the manufacturer include the I-V curve, open circuit voltage (V_{oc}), shunt circuit current (I_{sc}), and voltage (V_{mpp}), current (I_{mpp}), and power (P_{max}) at the maximum power point (MPP), measured at given Temperature under a standard AM 1.5 solar spectrum and irradiance of 100 mW/cm². To establish the solar cell model in Eq. (1), five parameters of the solar cell equation: R_s, R_{sh}, n, I_s and I_{ph} must be extracted using data provided by the manufacturer.

METHODS

- For most practical illuminated solar cells we usually consider that I_s << I_{ph}, the photocurrent can be given by the approximation I_{sc} ≈ I_{ph}, where I_{sc} is the short-circuit current. This approximation is highly acceptable and it introduces no significant errors in subsequent calculations^[19].
- The shunt conductance G_{sh} is evaluated from the reverse or direct bias characteristics by a simple linear fit^[20]. The calculated value of G_{sh} gives the shunt current I_p = G_{sh}V.
- The determination of ideality factor and the series resistance, Our measured I-V characteristics are corrected considering the value of the shunt conductance as obtained and for V+R_sI >> kT, the current voltage relation becomes:

$$I = I_{ph} - I_s \left[\exp\left(\frac{\beta}{n}(V + IR_s)\right) \right] \quad (2)$$

By writing relation (2) in its logarithmic form^[21].

$$Y = \frac{\beta}{n}(R_s + X) \quad \text{For } I \gg I_s \quad (3)$$

$$\text{With: } Y = \frac{1}{I - I_0} \ln \frac{(I_{ph} - I)}{(I_{ph} - I_0)} \quad \text{and} \quad X = \frac{(V - V_0)}{(I - I_0)}$$

And (V_0, I_0) is a point of the I-V curve.

The linear regression of equation (3) gives n and R_s , but when R_s is low or when multiple conduction processes intervene, the determination of R_s become difficult, so, to get a better accuracy we consider a set of I_i - V_i data giving rise to a set of X-Y values, with i varying from 1 to N . Then, we calculate X and Y values for $I_0 = I_{i0}$ and $I = I_{i0+1}$ up to $I = I_N$. This gives $(N-1)$ pairs of X-Y data. We start again with $I_0 = I_{i0+1}$ and $I = I_{i0+2}$ up to I_N and get $(N-2)$ additional X-Y data, and so on, up to $I_0 = I_{N-1}$. Finally, we obtain $N(N-1)/2$ pairs of X-Y data that means more values for the linear regression.

The most interesting point with this method is the fact that we do not have any limitation condition on the voltage hop and it is very easy to use.

At last, The saturation current I_s was evaluated using a standard method based on the I-V data by plotting $\ln(I_{ph} - I_{cr})$ versus V_{cr} equation (4). Note that I_{cr} - V_{cr} data were the corrected current voltage I-V data taking into account the effect of the series resistance where I-V are the measured current-voltage data.

When we plot $\ln(I_c)$ where $(I_c = I_{ph} - I_{cr})$ versus V_{cr} , it gives a straight line that yields I_s from the intercept with the y-axis.

RESULTS AND DISCUSSION

The current-voltage (I-V) characteristics of TiO_2 nanostructures DSSC is taken from the work of Jingbin et al. (2010) and The current-voltage (I-V) characteristics of ZnO nanotube is taken from the work of Fang Shoa et al. . The two characteristics correspond to the higher photovoltaic performance, where $\eta=6.00\%$, $FF=58.33\%$, $I_{sc}=15.25\text{mAcm}^{-2}$ and $V_{oc}=0.67\text{V}$ for TiO_2 nanostructures, and for ZnO nanotube $\eta=1.18\%$, $FF=0.58\%$, $I_{sc}=3.24\text{mAcm}^{-2}$ and $V_{oc}=0.68\text{V}$.

The extracted parameters obtained using the method proposed here for the Dye-Sensitized solar cell based on TiO_2 nanostructures and ZnO nanotube are given in Table 1, and to test the quality of the fit to the experimental data, the percentage error is calculated as follows:

$$e_i = (I_i - I_{i,cal}) (100 / I_i) \quad (4)$$

Where $I_{i,cal}$ is the current calculated for each V_i , by solving the implicit Eq.(1) with the determined set of parameters (I_{ph} , n , R_s , G_{sh} , I_s). (I_i, V_i) are respectively the measured current and voltage at the i_{th} point among N considered measured data points.

Statistical analysis of the results has also been performed. The root mean square error (RMSE), the mean bias error (MBE) and the mean absolute error (MAE) are the fundamental measures of accuracy. Thus, RMSE, MBE and MAE are given by:

$$\begin{aligned} RMSE &= \left(\sum |e_i|^2 / N \right)^{1/2} \\ MBE &= \sum e_i / N \\ MAE &= \sum |e_i| / N \end{aligned} \quad (5)$$

N is the number of measurements data taken into account.

Satisfactory agreement is obtained for most of the extracted parameters. Statistical indicators of accuracy for the method of this work are shown in Table 1.

Table1: Extracted parameters for Dye-Sensitized solar cell based on TiO₂ nanostructures and ZnO nanotube

	DSSC-TiO ₂ nanostructures	DSSC-ZnO nanotube
G _{sh} (Ω ⁻¹)	0.001269	0.000588
R _s (Ω)	0.025923	0.383441
n	1.629251	3.560949
I _s (μA)	0.33556	0.16553
I _{ph} (mA/cm ²)	15.99	3.25
RMSE	0.850353	1.875871
MBE	0.232276	0.727544
MAE	0.757886	1.053901

Figures 1 and 2 show the plot of I-V experimental characteristics and the fitted curves derived from equation (1) with the parameters shown in Table 1 for Dye-Sensitized solar cell based on TiO₂ nanostructures and ZnO nanotube.

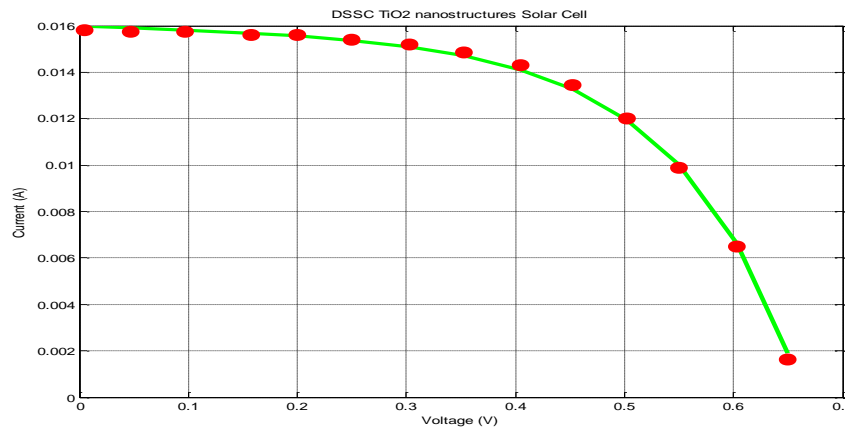


Figure 1: Experimental (●) data and fitted curve (-) of TiO₂ nanostructures DSSC.

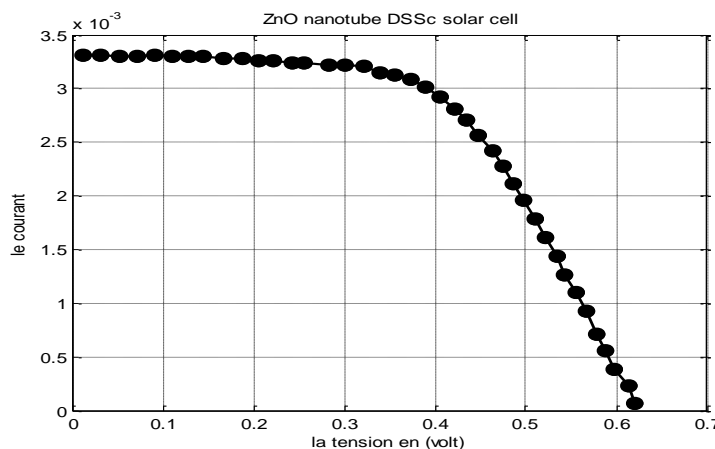


Figure 2: Experimental (●) data and fitted curve (-) of ZnO nanotube DSSC.

Extracting solar cells parameters is a vital importance for the quality control and evaluation of the performance of the solar cells, this parameters are: series resistance, shunt conductance, saturation current, the diode quality factor and the photocurrent. A simple method for extracting the solar cell parameters, based on the measured current-voltage data. The method has been successfully applied to dye-Sensitized solar cell based on TiO₂ nanostructures and ZnO nanotube under different temperatures.

Good agreement is observed for the different DSSCs, especially for the TiO₂ nanostructures solar cells with statistical error less than 1%, and 2% for ZnO nanotube DSSC solar cells respectively, which attribute mainly to lower parasitic losses, where we can observe a low series resistance 0.025923Ω compared to 0.383441 Ω for TiO₂ nanostructures and ZnO nanotube solar cell respectively.

The interesting point with the procedure described herein is relation between the results, where the five solar cells parameters extractions explain the difference in conversion efficient of the different DSSCs.

Effects of thickness on the output parameters

Figs. 3-4 show the effect of the geometry parameter (thickness) on output parameters: FF, I_{sc}, V_{oc}, η of dye-sensitized solar cells based on ZnO nanotube with different lengths. The shortcircuit photocurrent densities (I_{sc}) obtained with nanotubes of 0.7, 1.5, 2.9 and 5.1 μm lengths were 0.68, 1.51, 2.50 and 3.24 mA cm⁻², respectively. The highest photovoltaic performance of 1.18% (open-circuit voltage V_{oc} = 0.68 V and fill factor FF = 0.58) was achieved for the sample of 5.1 μm length. This efficiency is attractive, taking into account that the film thickness is only 5.1 μm and no scattering layer is added. The V_{oc} of the DSSC decreases upon increasing the length of the ZnO nanotubes, which is possibly related to the increase in the dark current which scales with the surface area of the ZnO film as shown by Jingbin et al.

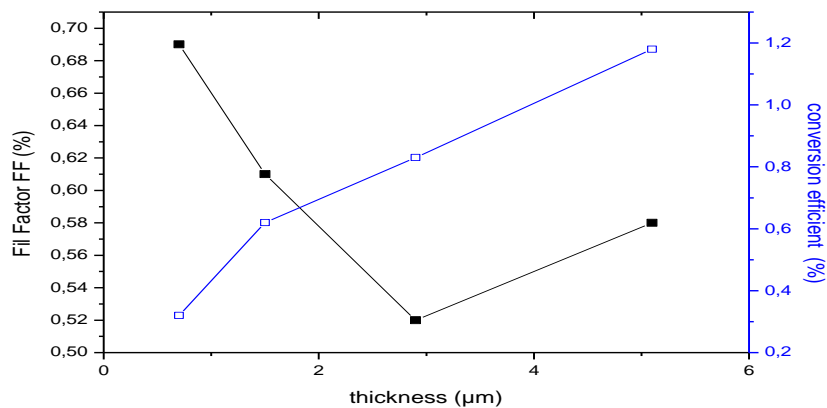


Figure 3: Effect of thickness on fill factor (FF) and conversion efficient of ZnO nanotube DSSC.

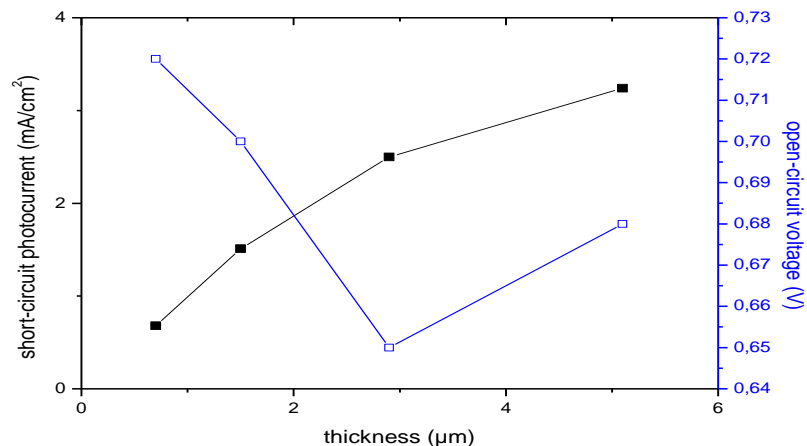


Figure 4: Effect of thickness on short-circuit photocurrent and open-circuit voltage of ZnO nanotube DSSC.

Figs. 5-6 show the effect of the geometry parameter (thickness) on output parameters: FF, I_{sc}, V_{oc}, η of dye-sensitized solar cells based on TiO₂ nanostructure grown in NaOH solution with different concentrations (0.5, 1, 3, and 10 M) and with different lengths. The shortcircuit photocurrent densities (I_{sc}) obtained with nanostructures of 11.68, 15.11, 24.10 and a (too thick to be measured) μm lengths were 10.26, 15.25, 10.2 and 3.71 mA cm⁻², respectively.

The highest photovoltaic performance of 6.00% (open-circuit voltage $V_{oc} = 0.67$ V and fill factor $FF = 58.33$) was achieved for the sample of $15.11 \mu\text{m}$ length^[22].

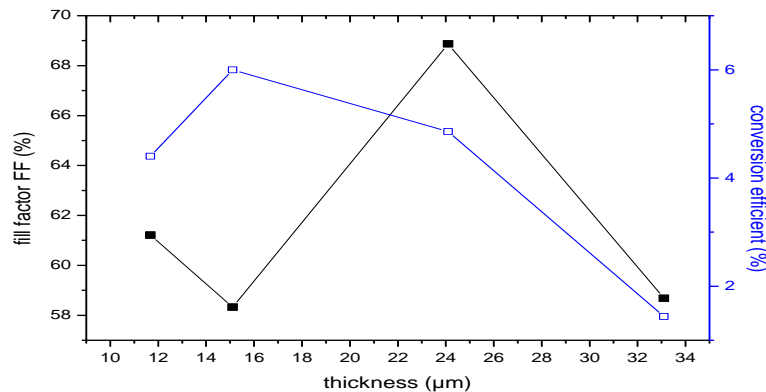


Figure 5: Effect of thickness on fill factor (FF) and conversion efficient of TiO_2 nanostructure DSSC.

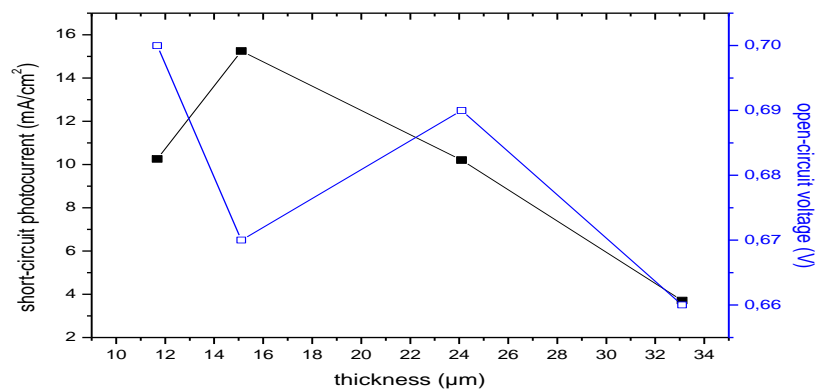


Figure 6: Effect of thickness on short-circuit photocurrent and open-circuit voltage of TiO_2 nanostructure DSSC.

The two DSSCs ZnO nanotube and TiO_2 nanostructure used (N719) dye sensitizer, The photon-current conversion efficiencies of DSSC using 0.7, 1.5, 2.9 and $5.1 \mu\text{m}$ length ZnO nanotubes were 0.32%, 0.62%, 0.83% and 1.18%, which were much lower than those of TiO_2 nanostructure DSSCs (i.e. 4.40%, 6.00%, 4.84% and 1.44%). So, the difference between the photovoltaic performance for these two type DSSCs is observed, where a high photovoltaic performance is given by TiO_2 Nanostructured with different thickness and over the range of NaOH concentrations, conversion efficient increased from 4.40% at 0.5M to a maximum value of 6.00% at 1 M, which correspond to a high short-circuit photocurrent densities 15.25 mA cm^{-2} . Compared with ZnO nanotube DSSC, where the higher conversion efficient is 1.18% correspond to high short-circuit photocurrent densities 3.24 mA cm^{-2} . The cause of this difference is the based materials properties (ZnO and TiO_2), the method of fabrication and the different condition of measured I-V characteristics of temperature and illumination. Where, ZnO is not an easy material, it's properties of which are greatly influenced by external conditions like synthesis methods, temperature, testing atmosphere air, vacuum or illumination, for example, minimal changes in the shape of the ZnO (nanoparticles, nanorods, nanotips, etc), can produce different properties which in turn, affects the interface with any organic semiconductor or dye molecule. In order, Titanium dioxide is a fascinating material, with a very broad range of different possible properties, which leads to its use in application as different as toothpaste additive.

CONCLUSION

In this contribution, a simple comparative study between experimental and simulation works to improve the deysensitized solar cell performance of two DSSCs based on TiO_2 nanostructures and ZnO nanotube, under different conditions of temperature. An evaluation of the physical parameters of solar cell: series resistance (R_s), ideality factor (n), saturation current (I_s), shunt resistance (R_{sh}) and photocurrent (I_{ph}) from measured current-voltage characteristics by using a numerical method proposed by the authors is presented by comparing the obtained results of two DSSCs, then we present the effect of geometric parameters on the output parameters which are: the conversion efficient, the

fill factor, the short-circuit photocurrent and the open-circuit voltage, where we observe a high photovoltaic performance for TiO₂ nanostructures with maximum conversion efficiency 6% compared to 1.18% for ZnO nanotube. Good results are given by the different DSSCs, and specially for on dye-sensitized TiO₂ nanostructures, which justify the experimental work.

ACKNOWLEDGMENTS

We would like to thank all the members of LESIMS laboratory, specially our supervisor Pr Djamel Eddine MEKKI for his advices and help and my wife Nadia Nehaoua for her comprehension and support.

REFERENCES

1. Gratzel M, perspectives for dye-sensitized nanocrystalline solar cells. *Prog Photovolt Res App.* 20008, 171.
2. Chen X B, Burda C, photoelectron spectroscopic investigation of nitrogen-doped titania nanoparticles. *J Phys Chem B.* 2004, 108, 15446.
3. Anusorn K, Kevin T, Kensuke T, Masaru K, Prashant VK. Quantum dot solar cells. Tuning photoresponse through size and shape control of CdSe-TiO₂ architecture. *J Am Chem Soc.* 2008;130(2):4007-4015.
4. Zhang J, Zhao Z, Wang X, Vu T, Guan J, Yu Z, Li Z, Zou Z. Increasing the oxygen density on the TiO₂ surface by La-doping for dye-sensitized solar cells. *J Phys Chem C.* 2010;114:18396.
5. Chiba Y, Islam A, Watanabe Y, Komiya R, Koide N, Han L, Dye-sensitized solar cells with conversion efficiency of 11.1%. *Jpn J Appl Phys.* 2002;45:L638.
6. Bauer C, Boschloo G, Mukhtar E, Hagfeldt A. Recombination in Ru(dcbpy)₂, sensitized nanostructured ZnO. *J Phys Chem B.* 2001;105:5585.
7. Myo Than HTAY, Minoru ITOH, Yoshio HASHIMOTO, Kentaro ITO. Photoluminescence properties and morphology of submicron-sized ZnO crystals prepared by ultrasonic spray pyrolysis. *J App. Phys.* 2008;47:541.
8. Quintana M, Edvinsson T, Hagfeldt A, Boschloo G. Comparison of dye-sensitized ZnO and TiO₂ solar cells: studies of charge transport and carrier lifetime. *J Phy Chem C.* 2007;111:1035.
9. Quintana M, Marinado T, Nonomura K, Boschloo G, Hagfeldt A. Organic chromophore-sensitized ZnO solar cells: electrolyte-dependent dye desorption and band-edge shifts. *J Photochem Photobiol A.* 2009;202:159.
10. Gonzalez Valls I, Lira-Cantu M. Vertically-aligned nanostructures of ZnO for excitonic solar cells. *Energy Environ Sci.* 2009;2:1.
11. Gratzel M, O'regan B. A low-cost high-efficiency solar cells based on dye-colloidal TiO₂ films. *Nature.* 1991; 353:737.
12. Yasuo Chiba, Ashraf Islam, Yuki watanabe, Ryoichi komiya, Naoki koide, Liyuan han. Dye-sensitized solar cells with conversion efficiency of 11.1%. *Jap J App Phy.* 2006;45(25):L638-L640.
13. Ozgur U, Alivov Y I, Liu C, Teke A, Reshchikov M A, Dogan S, et al. Comprehensive review of ZnO materials and devices. *J Appl Phys.* 2005;98:04131.
14. Pearton SJ, Norton DP, Ip K, Heo W, steiner T. Recent progress in processing and properties of ZnO. *Prog Mater Sci.* 2005;50:293-340.
15. Martinson ABF, Goes MS, Fabregat-Santiago, Bisquert FJ, Pellin MJ, Hupp JT. Electron transport in dye-sensitized solar cells based on ZnO nanotubes: evidence for highly efficient charge collection and exceptionally rapid dynamics. *J Phys Chem.* 2009;A113:4015-21.
16. Jiang CY, Sun XW, Lo GQ, Kwong DL, Wang JX. Improved dye-sensitized solar cells with ZnO nano flower photoanode. *Appl Phys Lett.* 2007;90:263501.
17. Hosono E, Fujihara S, Honma I, Zhou H. The fabrication of an upright-standing zinc oxide nanosheet for use in dye-sensitized solar cells. *Adv Mater.* 2005;17:2091-4.
18. Chiu WH, Lee CH, Cheng HM, Lin HF, Liao SC, Wu JM, et al. Efficient electron transport in tetrapod-like ZnO metal-free dye-sensitized solar cells. *Energy Environ Sci.* 2009;2:694-8.
19. Chegaar M, Azzouzi G, Mialhe P, simple parameter extraction method for illuminated solar cells. *Solid State Electronics.* 2006;50:1234-1237.
20. Chegaar M, Nehaoua N, Bouhemadou A. Organic and inorganic solar cells parameters evaluation from single I-V plot. *Energy conversion and management. Energy Conv Manag.* 2008;49:1376-1379.
21. Nehaoua N, Chergui Y, Mekki D E, determination of organic solar cell parameters based on single or multiple pin structure. *Vacuum.* 2010;84:326-329.
22. Fang shao, Jing sun, lian gao, Songwang, Jianqiang lu, growth of various TiO₂ nanostructure for dye sensitized solar cells. *Physical Chem C.* 2009.